Multipath-Assisted Single-Anchor Indoor Localization in an Office Environment

(Invited Paper)

Paul Meissner and Klaus Witrisal
Graz University of Technology, Graz, Austria, Email: {paul.meissner, witrisal}@tugraz.at

***Abstract*—Multipath propagation is one of the key problems for indoor localization systems. Strong multipath components can cause range estimates to anchor nodes to be severely biased. If a floor plan is available, reflected signal paths can be used effectively by mapping them to virtual anchors. We show how to make use of the rich localization information provided by just one anchor node. Using tracking algorithms both with and without data association, we achieve accurate and robust localization, which is verified in an indoor environment using measured data at ultra-wide bandwidths. With an extended Kalman filter and data association, a position error of 22 cm is obtained for 90 % of the estimates at a bandwidth of 2 GHz.**

I. Introduction

In prior work [1], we have introduced a multipath-assisted indoor localization and tracking scheme. Using a known floor plan, a single physical anchor node can be turned into a set of virtual anchors (VAs). Using ultra-wideband (UWB) signals, reflected signal paths are resolvable and provide rich localization information [2], [3]. In this contribution, we verify the performance of the scheme using measured data in an indoor environment. The results confirm the excellent accuracy observed in simulations previously and help to identify major influences on the system performance.

Signal reflections are also exploited in [4], but with the restriction to rectangular rooms and single reflections. In [5], VAs are used whose locations are unknown and exploited via cooperation. If reflected signal paths are used as measurement inputs for tracking algorithms like extended Kalman filters (EKFs) [6], the association of range estimates to features in the environment may be unknown. In this case, data association (DA) is necessary [7]. In [8], this is done by finding the nearest neighbor and most probable DAs. In our contribution, we show how the DA can be solved using optimal sub-pattern assignment [9], i.e. finding the subset of measurements that optimally fits to the expected environmental features. The associated measurements can be used as input for an EKF. As a direct comparison with our prior work in [1], a particle filter that can deal with complete lack of DA is also evaluated.

This paper is organized as follows: Section II introduces the scenario, the measurements and the geometric modeling, Section III deals with the extraction of multipath components (MPCs). Tracking algorithms are introduced in Section IV, their performance is discussed in Section V and Section VI draws conclusions.

This work was partly supported by the Austrian Science Fund (FWF) within the National Research Network SISE project S10604-N13, and by the Austria Research Promotion Agency (FFG) within KIRAS PL3, grant nb. 832335 "LOBSTER"

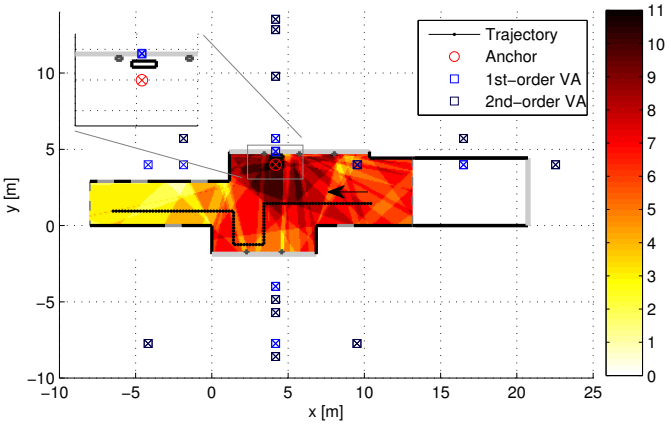

Fig. 1. Scenario with trajectory of a moving agent and physical as well as some of the virtual anchor nodes, with the number of expected virtual anchors N_k in color. The upper-left corner shows a close-up of the base station area.

II. Scenario, Measurements and Modeling

The indoor scenario is shown in Fig. 1. It is the ground floor of a multi-storey office building, in which our laboratory is situated. Black lines represent concrete walls, the gray ones are large windows and metal doors. The building further extends several tens of meters to the left. We performed channel measurements over the shown trajectory consisting of 220 points spaced by 10 cm. At each point, the UWB channel was measured with a Rhode & Schwarz ZVA-24 vector network analyzer over a frequency range of $3.1 - 10.6$ GHz. The obtained channel transfer functions are transformed to time domain via an inverse discrete Fourier transform. An outline of this procedure and a more detailed description and analysis of the measurement campaign can be found in [2].

Our aim is to localize and track a moving agent node with the help of just a single base station together with the signal reflections in the building walls [1]. Assuming that these MPCs are resolvable in the channel impulse response (CIR), they can be mapped to VAs, which are mirror images of the anchor node with respect to the corresponding reflecting surface. Hence, if the floor plan is known, one physically existing anchor can be turned into a set of VAs usable for localization. The set of all VAs over the whole floor plan is denoted as

$$\mathcal{A} = \{\mathbf{a}_i \ : \ i = 1, \ldots, N_{\mathrm{VA}}\}. \tag{1}$$

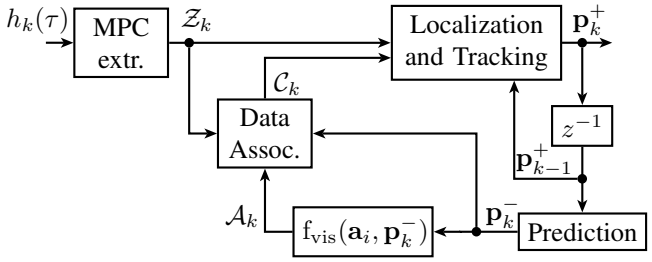

Fig. 2. Overview of localization and tracking scheme.

The geometric visibility region of the i-th VA, which is at position $\mathbf{a}_i$, can be pre-computed using ray-tracing, as outlined in [2]. In this contribution, this is denoted with a function

$$f_{\mathrm{vis}}(\mathbf{a}_i, \mathbf{p}) = \begin{cases} 1, & \text{if VA } \mathbf{a}_i \text{ is visible at } \mathbf{p} \\ 0, & \text{else.} \end{cases} \tag{2}$$

Evaluating this function for all VAs at the k-th position $\mathbf{p}_k$ yields the set of expected visible VAs at this position, which is denoted as

$$\mathcal{A}_k = \{\mathbf{a}_{k,1}, \ldots, \mathbf{a}_{k,N_k}\} = \{\mathbf{a}_i \ : \ f_{\mathrm{vis}}(\mathbf{a}_i, \mathbf{p}_k) = 1\}. \tag{3}$$

Hence, $\mathcal{A}_k$ is only a subset of $\mathcal{A}$ with cardinality $|\mathcal{A}_k| = N_k$. Fig. 1 shows N_k over the floor plan, where single- and double-reflections are taken into account in the construction of $\mathcal{A}$. We observe a potential challenge for multipath-assisted localization: The set of anchors that can be used for position estimation rapidly changes over the area. Hence, an agent moving through the scenario needs some awareness of the currently valid set of VAs to perform location estimation.

III. Multipath extraction and localization

Fig. 2 shows the conceptual layout of our proposed multipath-assisted localization scheme. Localization and tracking algorithms use range estimates to the VAs, which are delivered by an MPC-extraction step. As this step is performed without any location information, it extracts the arrival times of the M_k largest local maxima from the CIR.

The UWB CIR $h_k(\tau)$ is modeled as

$$h_k(\tau) = \sum_{l=1}^{L_k} \alpha_{k,l}\delta(\tau - \tau_{k,l}) + \nu_k(\tau) + n_k(\tau). \tag{4}$$

It consists of L_k MPCs caused by deterministic reflections, with corresponding amplitudes $\alpha_{k,l}$ and delays $\tau_{k,l}$. The signal $\nu_k(\tau)$ models diffuse scattered components and $n_k(\tau)$ is the measurement noise. We expect that at position $\mathbf{p}_k$, the VAs in $\mathcal{A}_k$ are responsible for a part of the deterministic reflections, i.e. $N_k \leq L_k$. Results in [2] show that these MPCs carry a significant part of the energy of the CIR, which justifies our choice to extract the arrival times of the local maxima.

The set of M_k estimated path delays is denoted as $\mathcal{Z}_k = \{z_{k,1}, \ldots, z_{k,M_k}\}$, where $z_{k,i} = c\tau_{k,i}$ and c is the propagation velocity. Of course $\mathcal{Z}_k$ does not only contain range estimates to the VAs in $\mathcal{A}_k$, but also entries that are due to noise or diffuse scattered components, i.e. clutter. The quality of $\mathcal{Z}_k$ is determined by its distance to the ground truth $\mathcal{D}_k$, which is the set of distances to the expected VAs at $\mathbf{p}_k$, i.e.

$$\mathcal{D}_k = \{d_{k,1}, \ldots, d_{k,N_k}\} = \{d(\mathbf{a}_i, \mathbf{p}_k) \ : \ \mathbf{a}_i \in \mathcal{A}_k\} \tag{5}$$

where $d(\mathbf{a}_i, \mathbf{p}_k)$ is simply the Euclidean distance between the VA $\mathbf{a}_i$ and the point $\mathbf{p}_k$. However, as both $\mathcal{Z}_k$ and $\mathcal{D}_k$ are sets of usually different cardinality, no straightforward distance measure is available. Instead, we resort to a popular *multi-target miss-distance*, the optimal sub-pattern assignment (OSPA) metric [9]. For $M_k \geq N_k$, which can be ensured by filling up $\mathcal{Z}_k$ with dummy clutter, it is defined as

$$d_{\mathrm{OSPA}}(\mathcal{D}_k, \mathcal{Z}_k) = \left[\frac{1}{M_k}\left(\min_{\boldsymbol{\pi}\in\Pi_{M_k}} \sum_{i=1}^{N_k} d^{(d_\mathrm{c})}(d_{k,i}, z_{k,\boldsymbol{\pi}_i})^p + d_\mathrm{c}^p(M_k - N_k)\right)\right]^{1/p} \tag{6}$$

where Π_{M_k} is the set of permutations of positive integers up to M_k. The function $d^{(d_\mathrm{c})}(x, y) = \min(d_\mathrm{c}, d(x, y))$, i.e. an arbitrary distance metric $d(\cdot)$ that is cut off at a $d_\mathrm{c} > 0$, which is a design parameter. The first part of the metric, the sum, is the cumulative distance over the optimal sub-pattern assignment of $\mathcal{Z}_k$ to $\mathcal{D}_k$, i.e. where N_k entries of Z_k are assigned optimally to the entries of $\mathcal{D}_k$. The Hungarian algorithm is used for this assignment [10]. For the remaining $M_k - N_k$ entries of $\mathcal{Z}_k$, d_c is assigned as penalty distance.

IV. Tracking and Data Association

The motion of the agent is modeled with a standard discrete-time linear state-space model as in [1]

$$\mathbf{x}_{k+1} = \begin{bmatrix} 1 & 0 & \Delta T & 0 \\ 0 & 1 & 0 & \Delta T \\ 0 & 0 & 1 & 0 \\ 0 & 0 & 0 & 1 \end{bmatrix} \mathbf{x}_k + \begin{bmatrix} \frac{\Delta T^2}{2} & 0 \\ 0 & \frac{\Delta T^2}{2} \\ \Delta T & 0 \\ 0 & \Delta T \end{bmatrix} \mathbf{n}_{\mathrm{a},k} \tag{7}$$

where the state vector $\mathbf{x}_k = [p_x, p_y, v_x, v_y]_k^T$ contains position and velocity components in $x-$ and $y-$direction, ΔT is the update interval and $\mathbf{n}_{\mathrm{a},k}$ is acceleration noise. For range-based tracking using the VAs, we use $\mathcal{Z}_k$ as measurement input for the tracking algorithm at time-step k. However, the association of the entries of $\mathcal{Z}_k$ to the VAs is unknown [7]. Therefore, we introduce a set $\mathcal{C}_k$ of correspondence variables [6], whose i-th entry $c_{k,i}$ is defined as

$$c_{k,i} = \begin{cases} j, & \text{if } z_{k,i} \text{ corresponds to VA } \mathbf{a}_j \ (j = 1, \ldots, N_{\mathrm{VA}}) \\ 0, & \text{if } z_{k,i} \text{ corresponds to clutter.} \end{cases} \tag{8}$$

A. Extended Kalman filter with data association (EKF-DA)

If $\mathcal{C}_k$ is available, state-space estimation can be performed by e.g. an EKF using the linear motion model and a linearized observation model [6] based on the associated entries of $\mathcal{Z}_k$ and the corresponding VAs. As the well-known EKF equations are used, we concentrate on the description of the DA here. Fig. 2 depicts the general scheme: Assuming

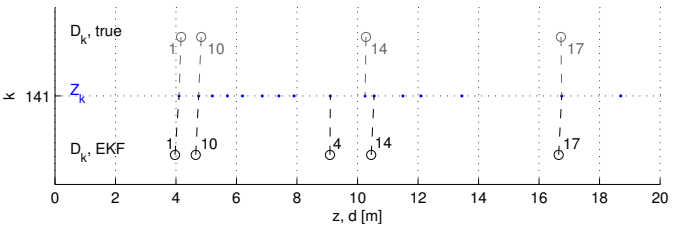

Fig. 3. Example for the DA for a bandwidth of 2 GHz at $k = 141$, zoomed view on x-axis. Upper part shows the genie-aided DA, lower part the DA based on the estimated position. Due to the position error, the EKF expects a different set $\mathcal{D}_k$. For the VA at $\mathbf{a}_4$, a clutter measurement is associated, for $\mathbf{a}_{14}$, the wrong measurement is associated.

the EKF is already on track at time step k, the predicted position $\mathbf{p}_k^-$ is computed using the motion model (7) and the previous posterior estimate $\mathbf{p}_{k-1}^+$. Using $f_{\text{vis}}(\mathbf{a}_i, \mathbf{p}_k^-)$, the set of expected VAs $\mathcal{A}_k$, and subsequently the expected delays $\mathcal{D}_k$ are estimated.

Inspired by the definition of the OSPA metric, the DA is done using optimal sub-pattern assignment between $\mathcal{D}_k$ and $\mathcal{Z}_k$, which is reflected in the first part of (6)

$$\boldsymbol{\pi}_{\text{opt}} = \arg \min_{\boldsymbol{\pi} \in \Pi_{M_k}} \sum_{i=1}^{N_k} d^{(d_c)}(d_{k,i}, z_{k,\boldsymbol{\pi}_i})^p. \tag{9}$$

The first N_k entries of $\boldsymbol{\pi}_{\text{opt}}$ contain the indices of those entries of $\mathcal{Z}_k$ that have been optimally assigned to $\mathcal{D}_k$. For some entries of $\mathcal{D}_k$, we will probably have $d^{(d_c)}(d_{k,i}, z_{k,\boldsymbol{\pi}_{opt,i}}) = d_c$, i.e. this expected distance has an assigned measurement, but the difference between measurement and expected distance is larger or equal to the cutoff distance. We expect that by using UWB signals, the estimated path delays will be quite accurate, provided that they are detected. Hence, we select a certain d_c that may depend on the bandwidth and reject the corresponding assignments as outliers. Formally, the DA is expressed by setting the correspondence variables as

$$c_{k,i} = \begin{cases} j, & \text{if } \boldsymbol{\pi}_j = i \text{ and } d^{(d_c)}(d_{k,j}, z_{k,i}) < d_c \\ 0, & \text{else} \end{cases} \tag{10}$$

B. Extended Kalman filter with genie-aided data association (EKF-GADA)

It is well-known that erroneous DA can lead to catastrophic failures of Kalman filters. Hence we propose a genie-aided DA procedure that can act as a benchmark for other trackers. The only difference to the DA procedure explained in Sec. IV-A is that here the set of expected path delays $\mathcal{D}_k$ is calculated based on the true position $\mathbf{p}_k$.

C. Particle filter without data association

We compare the performance of the EKF with a particle filter-based tracker (PF) that was introduced in [1]. This filter has the advantage of not requiring DA. N_p particles are initially selected randomly over the floor plan. In each time-step, they are propagated through the motion model (7) and subsequently weighted and resampled according to their

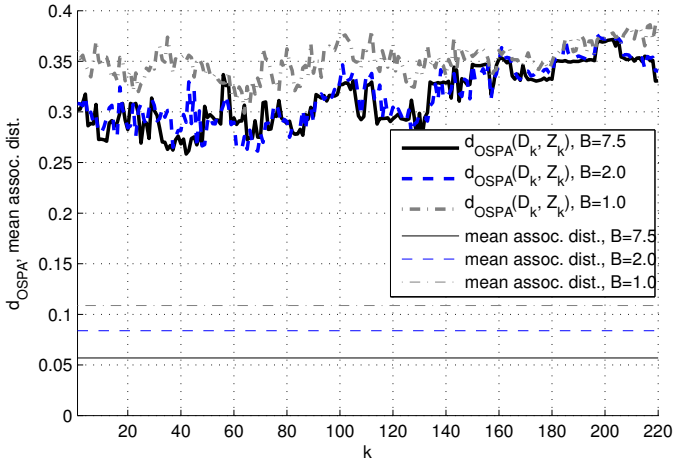

Fig. 4. OSPA metric over the trajectory for different bandwidths as well as mean distance of associated path delays.

likelihood with respect to the current measurement. For a particle at $\mathbf{p}_k$ and a range estimate $z_{k,i}$, the likelihood is

$$\begin{aligned} p(z_{k,i}|\mathbf{p}_k) = P_{\text{VA}} \sum_{n=1}^{N_{\text{VA}}} P_{\text{v},n} f_{\text{vis}}(\mathbf{a}_n, \mathbf{p}_k) p(z_{k,i}|\mathbf{p}_k, c_{k,i} = n) \\ + (1 - P_{\text{VA}}) p(z_{k,i}|\mathbf{p}_k, c_{k,i} = 0) \end{aligned} \tag{11}$$

where $P_{\text{v},n}$ is the visibility probability of the n-th VA and P_{VA} is the probability that $z_{k,i}$ is caused by any of the VAs. The likelihood is a sum over all possible causes of $z_{k,i}$, i.e. over all VAs visible at $\mathbf{p}_k$ and also the possibility that $z_{k,i}$ is clutter. The corresponding conditional densities of $z_{k,i}$ are selected as Gaussian with mean equal to the true distance in the first case, and as uniform over the range from zero to a maximum range value in the latter case. Treating $\mathcal{Z}_k$ as a random vector, the joint likelihood of all measurements is calculated as the product of the individual likelihoods (11). This assumes that the $z_{k,i}$ are independent, which is a simplification resulting in severe multimodality, as discussed in [1].

V. Performance Results

The performance of the proposed tracking algorithms is evaluated over the scenario in Fig. 1. We selected the full bandwidth of $B = 7.5$ GHz as well as bandwidths of 2 GHz and 1 GHz, where the frequency range of the reduced bandwidths starts at 6 GHz. For the MPC-extraction, the $M_k = 20$ largest local maxima are extracted from $|h_k(\tau)|$, using the subtraction method discussed in [2]. The EKFs are provided with a perfect initialization. In practice, initialization can be handled using a Gaussian sum filter, as described in [1].

Fig. 3 shows an example for the DA procedure for $B = 2$ GHz at a point on the trajectory. The cutoff distance has been chosen as $d_c = 0.4$ m. Although the true position $\mathbf{p}_k$ and the EKFs estimate of it are just 14 cm apart, the set of expected VAs differ. This leads to an erroneous detection of the VA at $\mathbf{a}_4$, where a clutter measurement is within the cutoff distance. Also the association for VA $\mathbf{a}_{14}$ is wrong due to the

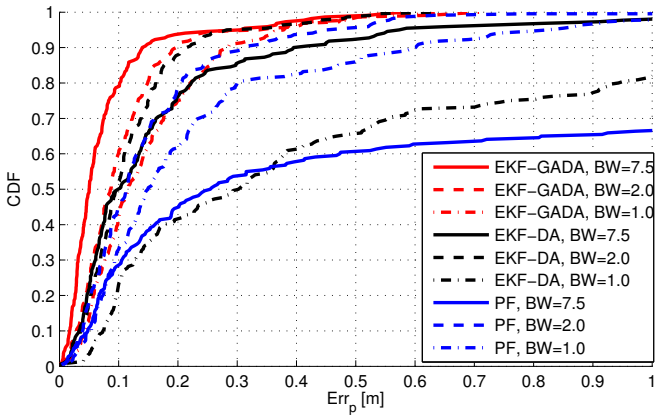

Fig. 5. CDFs of the position error for the proposed tracking algorithms and different bandwidths.

slight postion error. This erroneous example has been chosen on purpose to highlight potential error sources, in general the DA based on optimal sub-pattern assignment works stable with a sensitivity tunable via the choice of d_c.

Fig. 4 shows the OSPA metric defined in (6) over the trajectory for all bandwidths and $d_c = 0.4\,\text{m}$. It can be observed that for $B = 7.5\,\text{GHz}$ and $B = 2\,\text{GHz}$, the OSPA distance qualitatively shows similar behavior. For $B = 1\,\text{GHz}$, the distance is larger, which is partly because of the higher probability of path overlap [3]. Using the optimal sub-pattern assignment, a measurement can only be assigned to one VA, whereas it might be caused by multiple ones. Due to the fact the MPC extraction returns the 20 largest local maxima and the mean N_k is around 5.6, the cardinality error dominates the metric. Therefore, also the mean distance over the trajectory of the associated sub-pattern is shown, as this also corresponds to the objective function for the DA in (9). Here, the beneficial influence of a high bandwidth is clearly visible.

The performance of the tracking algorithms is compared in Fig. 5, which shows CDFs of the position error. The influence of bandwidth is interesting: The EKF-GADA does not suffer from erroneous associations and can thus make use of the large bandwidth that also results in low probability of path overlap. The latter is problematic for the EKF-DA at $B = 1\,\text{GHz}$, as every measurement can only be associated once, causing increased sensitivity to miss-associations. For the EKF-DA at $B = 2\,\text{GHz}$, a promising $90\,\%$ of the estimates are within $22\,\text{cm}$. For the higher bandwidth, the DA gets trickier: The MPC extraction returns more clutter around the true MPCs, as at this bandwidth, diffuse tails of some MPCs can be resolved. For the PF at this bandwidth, this clutter leads to pronounced maxima of the multimodal likelihood function in the vicinity of the true position. This can draw the PF estimate away from the true trajectory. For the lower bandwidths, this effect is less pronounced and the PF offers reasonable performance.

Qualitatively, the performance is shown in Fig. 6 for $B = 2\,\text{GHz}$. For this case, the EKF-DA approaches the EKF with genie-aided DA. Near the end of the trajectory, all filters are

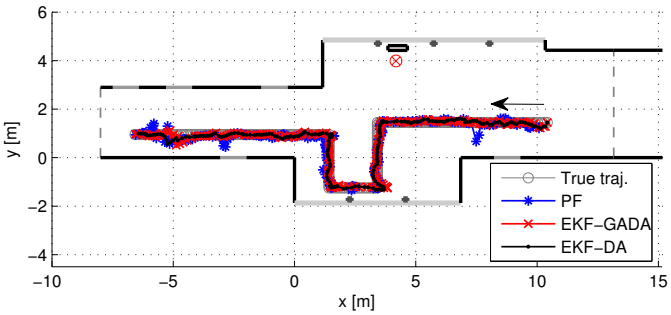

Fig. 6. Performance of proposed algorithms over scenario for BW=2 GHz.

drawn away from the trajectory, as in this region, only two VAs are visible. All the filters can again lock on the trajectory once the double reflection between the corridor walls becomes visible. Also the influence of geometric dilution of precision is visible at the second bend of the trajectory. Both EKFs tend to the wrong direction initially and the variance in x-direction increases. This is due to the fact that in this region, only VAs on a vertical line through the anchor are visible, providing little information in x-direction [3].

VI. Conclusion and Outlook

We have presented an indoor localization scheme with only a single base station that effectively makes use of multipath propagation. Using a known floor plan and the concept of virtual anchors, excellent performance can be achieved with tracking algorithms, also in the absence of data association information. Data association based on optimal sub-pattern assignment can further improve the accuracy, even if the clutter rate is high. In future work, tracking of the multipath components themselves will be used to significantly reduce clutter and to help in resolving path overlap problems.

References

[1] P. Meissner, T. Gigl, and K. Witrisal, "UWB Sequential Monte Carlo Positioning using Virtual Anchors," in *Proc. 2010 International Conference on Indoor Positioning and Indoor Navigation, IPIN, Zurich*, 2010.

[2] P. Meissner, D. Arnitz, T. Gigl, and K. Witrisal, "Analysis of an Indoor UWB Channel for Multipath-Aided Localization," in *2011 IEEE International Conference on Ultra-Wideband (ICUWB 2011)*, 2011.

[3] K. Witrisal and P. Meissner, "Performance Bounds for Multipath-aided Indoor Navigation and Tracking (MINT)," in *International Conference on Communications (ICC)*, 2012, accepted.

[4] V. La Tosa, B. Denis, and B. Uguen, "Joint Anchor-less Tracking and Room Dimensions Estimation through IR-UWB Peer-to-peer Communications," in *2011 IEEE International Conference on Ultra-Wideband (ICUWB 2011)*, 2011.

[5] Y. Shen and M. Win, "On the Use of Multipath Geometry for Wideband Cooperative Localization," in *Global Telecommunications Conference, 2009. GLOBECOM 2009. IEEE*, 2009, pp. 1 –6.

[6] S. Thrun, W. Burgard, and D. Fox, *Probabilistic Robotics*. MIT, 2006.

[7] Y. Bar-Shalom and T. Fortmann, *Tracking and Data Association*. Academic Press, 1988.

[8] T. Deissler and J. Thielecke, "UWB SLAM with Rao-Blackwellized Monte Carlo data association," in *Indoor Positioning and Indoor Navigation (IPIN), 2010 International Conference on*, sept. 2010, pp. 1 –5.

[9] D. Schuhmacher, B.-T. Vo, and B.-N. Vo, "A Consistent Metric for Performance Evaluation of Multi-Object Filters," *Signal Processing, IEEE Transactions on*, vol. 56, no. 8, pp. 3447 –3457, 2008.

[10] J. Munkres, "Algorithms for the Assignment and Transportation Problems," *Journal of the Society for Industrial and Applied Mathematics*, vol. 5, no. 1, pp. pp. 32–38, 1957.